

# Geminal Bis-ureas as Gelators for Organic Solvents: Gelation Properties and Structural Studies in Solution and in the Gel State

Franck S. Schoonbeek,<sup>[a]</sup> Jan H. van Esch,\*<sup>[a]</sup> Ron Hulst,<sup>[b]</sup> Richard M. Kellogg,<sup>[a]</sup> and Ben L. Feringa\*<sup>[a]</sup>

**Abstract:** Several geminal bis-urea compounds were synthesised by means of an acid-catalysed condensation of various benzaldehydes with different monoalkylureas. Many of these compounds form thermoreversible gels with a number of organic solvents at very low concentrations (<3 mM) and which are stable to temperatures higher than 100 °C. Electron microscopy revealed a

three-dimensional (3D) network of intertwined fibres, which are several tens of micrometers long and have a width ranging from approximately 30 to 300 nm. The possible aggregate forms

**Keywords:** aggregation • gels • hydrogen bonds • molecular modelling • self-assembly

and aggregate symmetries were evaluated by means of molecular mechanics calculations. <sup>1</sup>H NMR, 2D NMR, <sup>13</sup>C NMR and <sup>13</sup>C-CP/MAS NMR techniques were used to obtain information about the aggregation and possible aggregate symmetry of geminal bis-ureas in solution, in the gel state, and in the solid state.

## Introduction

Low molecular weight organic gelling agents are currently the subject of much attention, not only because of the numerous applications of gels, but also because gelation phenomena by low molecular weight organic gelling agents are still poorly understood.<sup>[1, 2, 3]</sup> These organogelators have in common that in organic solvents they self-assemble into long fibre-like structures through highly specific noncovalent interactions, such as hydrogen bonding and  $\pi$ - $\pi$  stacking. These fibres then entangle to form a three-dimensional (3D) network which retains the solvent within the pores through capillary forces. The molecular structures of known (very potent) organogelators are, however, very diverse, and often structurally closely related compounds do not exhibit any gelation properties. Most of the research has thus focussed on the exploration of the molecular diversity of organogelators, but many of these studies are hampered by the lack of knowledge on the self-assembly properties of the compounds under study.

A different approach towards a better understanding of organogels and the elucidation of the molecular prerequisites

for gelation is by the design of novel organogelators. Recently, Hanabusa et al. and our group independently demonstrated that bis-urea compounds are exceptionally well-suited for the design of low molecular weight gelators owing to the rigidity, strength and high directionality of the multiple intermolecular hydrogen bonds that can be formed.<sup>[4, 5]</sup> A key feature in the design of novel gelators appeared to be unidirectional gelator-gelator interactions, as is most clearly the case in *trans*-1,2-cyclohexyl- and 1,2-phenyl-bis(ureido) gelators.<sup>[6]</sup> The proximity of the urea groups in these gelating scaffolds, leads to adoption of a coplanar orientation, which strongly favours one-dimensional aggregation through hydrogen-bond formation (Figure 1). However, molecular modelling studies and experimental results indicate that one-dimensional aggregation by these compounds is prone to polymorphism, although the 1,2-bis(urea)cyclohexane and 1,2-bis(urea)benzene gelating scaffolds have little conformational freedom and the actual or dominant aggregate structure in the gels is not known in detail. So the problem that is faced is not trivial: is it possible to establish a clear relationship between crystal structure, gel structure, aggregation in solution and monomer structure? Reports on crystal structures of gelator molecules have been scarce up to now, and we were able to demonstrate in one case that the arrangement of gelator molecules in the crystal does not correspond fully with the molecular arrangement in a gel.<sup>[6b, 7, 8]</sup>

In the present work we turned our attention to the aggregation behaviour and gelation capability of novel geminal bis-urea compounds. For geminal bis-ureas it is expected that the two urea fragments do not have much

[a] Dr. J. H. van Esch, Prof. Dr. B. L. Feringa, F. S. Schoonbeek, Prof. Dr. R. M. Kellogg  
Department of Organic and Molecular Inorganic Chemistry Stratingh Institute, University of Groningen, Nijenborgh 4  
9747 AG Groningen (The Netherlands)  
Fax: (+31)50-363-4296  
E-mail: esch@chem.rug.nl  
feringa@chem.rug.nl

[b] Dr. R. Hulst  
Department of Chemical Analysis, University of Twente P.O. Box 217,  
7500 AE Enschede (The Netherlands)

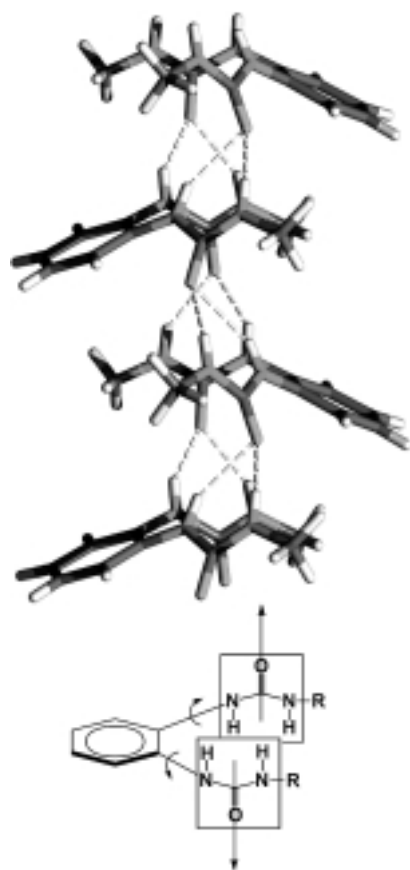


Figure 1. Conformational freedom in a 1,2-bis(urea)benzene derivative and X-ray structure of a 1,2-bis(urea)benzene in the solid state,<sup>[6b]</sup> clearly showing the presence of linear hydrogen-bonded aggregates in the solid state.

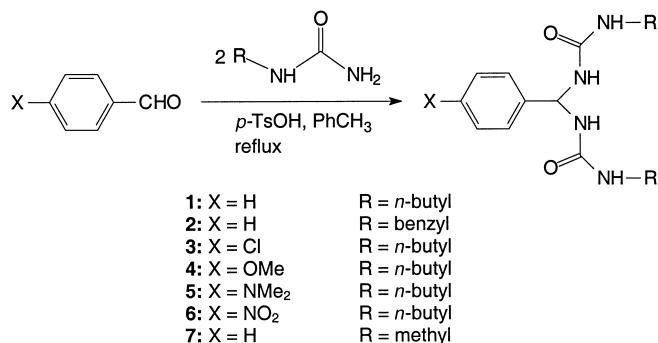
independent rotational freedom owing to their proximity, as demonstrated for 1,2-bis(urea)cyclohexane and 1,2-bis(urea)benzene derivatives. It is extremely likely that the hydrogen-bonding ability is directed along one intermolecular axis and therefore should strongly favour one-dimensional aggregation. The possible gelation of organic solvents by geminal bis-urea compounds will thus strengthen the concept of unidirectional interactions as a prerequisite for gelation. This knowledge will be valuable in the elucidation of the structural requirements for gelation by other types of gelling agents for which a first approximation of the directionality of intermolecular interactions is less well defined as with the hydrogen-bonding systems in the bis-urea compounds.

The second aim of our research on geminal bis-ureas is to obtain insight in to the relationship between conformation and aggregation. Here we report on the synthesis of geminal bis-urea compounds and their gelation capability for organic solvents, we also report on molecular modelling, and solution and solid-state NMR studies on their aggregation behaviour in solution and on the structure of the gels.

## Results and Discussion

**Synthesis:** The synthesis of compounds **1–6** was based on a literature procedure for the preparation of geminal bis-

acetamides.<sup>[9]</sup> This entails an, in principle, rather straightforward acid-catalysed condensation of a benzaldehyde and the desired monoalkylurea in refluxing toluene with azeotropic removal of water (Scheme 1). In most cases, however, a gel



Scheme 1. Synthesis of geminal bis-ureas **1–6**.

was formed during the reaction, and 100% conversion to the desired product was prevented. A decrease in the concentration of the reactants solved this problem for most of the systems studied. Upon cooling of the reaction mixture a precipitate or gel-like solid was formed, which could easily be isolated from the reaction mixture by filtration with suction.

Attempts to synthesise bis-ureas with longer alkyl chains (octyl, dodecyl) were not successful. Although inspection of samples from these reaction mixtures by <sup>1</sup>H NMR spectroscopy revealed that most of the starting materials had disappeared, no product precipitated from the reaction mixture upon cooling to room temperature, and all attempts to isolate the products by other means failed. The most likely explanation is that these geminal bis-ureas are very sensitive to the combination of traces of acid and moisture. For example, dissolving samples of **1–6** in commercial CDCl<sub>3</sub> (which contains traces of water and HCl) results in partial or complete decomposition into the parent aldehyde and alkyl-urea. In pure, acid-free CDCl<sub>3</sub> and in [D<sub>6</sub>]DMSO (which does contain some water but no acid) this problem does not exist.

**Gelation of organic solvents:** The gelating ability of geminal bis-urea compounds **1–6** for a range of organic solvents was examined (with the exception of **5**, which turned out to be too unstable with respect to hydrolysis) by dissolving approximately 10 mg of compound in 1 mL of the desired solvent under heating. The solubility of these compounds at room temperature (RT) is very poor in most solvents (chloroform is a notable exception). Upon cooling to room temperature, a gel, a precipitate or a clear solution was observed, depending on the solvent used. In the case of **1**, if gelation occurred, the concentration was gradually lowered until the gelating ability had disappeared. The results are summarised in Table 1 and show that a gelator concentration range of 3–15 mM is typical, this has also been found for other bis-urea compounds and many other organogelators.<sup>[1, 4, 6]</sup> Apparently these values represent a lower limit, at which the concentration of these aggregates is high enough and/or at which the size of the various aggregates in solution is large enough to sustain a 3D

Table 1. Gelation properties and critical gelator concentrations.<sup>[a]</sup>

Solvent	Compound				
	1	2	3	4	6
hexadecane	< 3	p	g	p	i
cyclohexane	< 3	p	g	g	g
toluene	< 5	p	s	g	g
<i>p</i> -xylene	< 5	p	s	g	g
tetralin	< 15	p	s	g(t)	g
<i>n</i> -butylacetate	< 5	p	s	p	p
1,2-dichloroethane	< 15	p	s	g	p
chloroform	s	s	s	s	s
dibutyl ether	< 15	p	g	g	p
acetonitrile	p	p	g	s	p
2-octanol	s (d)	s (d)	s (d)	s (d)	s (d)
2-propanol	s (d)	s (d)	s (d)	s (d)	s (d)
ethanol	s (d)	s (d)	s (d)	s (d)	s (d)
DMSO	s	s	s	s	s
cyclohexanone	p	s	s	s	p

[a] Critical gelator concentrations are given in mM. The following abbreviations are used: d, decomposition; g, gel; i, insoluble; p, precipitate; s, soluble; t, thixotropic.

network that retains the solvent, and results in the formation of a gel.<sup>[1]</sup>

From Table 1 it is clear that only **2** is not an effective gelator, this may be because the butyl groups in the other compounds are much more flexible than the benzyl groups present in **2**, and an increased tendency of **2** to crystallise or precipitate results, rather than gel formation. It is also clearly demonstrated that none of the compounds **1–6** gelate or precipitate in the tested protic solvents. NMR analysis of the solutions revealed that in these solvents **1–6** easily decompose to an acetal and monoalkylurea, both of which are soluble in protic solvents.

The gels given in Table 1 are stable for at least a few weeks at room temperature. In some solvents (hexadecane, cyclohexane) the gels are very turbid and are destroyed easily by mechanical agitation, whereas in tetralin, *p*-xylene and toluene the gels are completely transparent and stable towards agitation. The gel from the methoxy-substituted compound **4** in tetralin is thixotropic, that is, upon shaking, the gel loses its rigidity and becomes free flowing. Upon standing at rest for a few minutes the gel properties returned completely. This process can be repeated many times.

In all cases gelation was found to be completely thermo-reversible. Differential scanning calorimetry (DSC) of a tetralin gel of **1** (80 mM) gave a very broad melting endotherm ( $T_{\text{onset}} = 90^\circ\text{C}$ ,  $T_{\text{max}} = 119^\circ\text{C}$ ,  $T_{\text{end}} = 130^\circ\text{C}$ ) with an enthalpy change of  $+65 \text{ kJ mol}^{-1}$ . This enthalpy corresponds well with gelation enthalpies reported previously for bis-urea gelators in various solvents,<sup>[4, 5a]</sup> and is about twice as large as the value that is found for breaking up large aggregates of mono-urea compounds in an apolar medium.<sup>[10]</sup> The broad temperature range of the melting process is indicative of a less cooperative phase transition.

The relationship between gelator concentration and melting point of the gel was studied in tetralin by the dropping ball method (Figure 2).<sup>[11]</sup> The melting point determined by the dropping ball method lies approximately  $10^\circ\text{C}$  below the maximum of the DSC melting endotherm, and therefore the evaluation of these data by a phase-separation model or

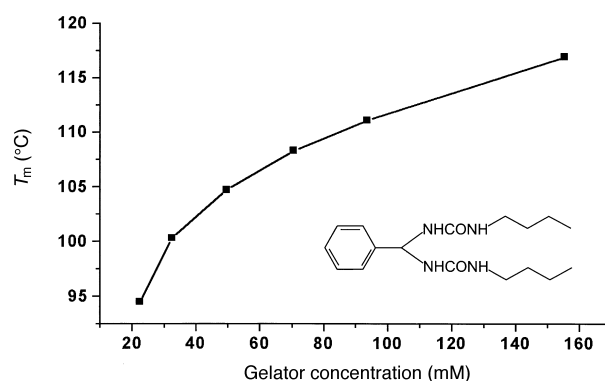


Figure 2. Melting points of a tetralin gel of **1** as determined by the dropping ball method.

Schraders equation, which describes ideal solubility behaviour, is not justified.<sup>[12, 13, 14]</sup> Furthermore, a gradual weakening of the gel is observed by the dropping ball method rather than a discrete phase transition, in complete agreement with the results from the DSC experiments.

Light microscopy shows that gels of **1** are birefringent (indicative of anisotropic properties), as was the case with previously reported linear bis-ureas, but further structural details cannot be seen. Electron microscopy (EM) reveals that compound **1** is able to aggregate into long, intertwining bundles of fibres which are occasionally split up and fused with other fibre bundles (junction zones), thus showing that the network does not result from purely mechanical contacts between the various fibres (Figure 3). The elongated shape of

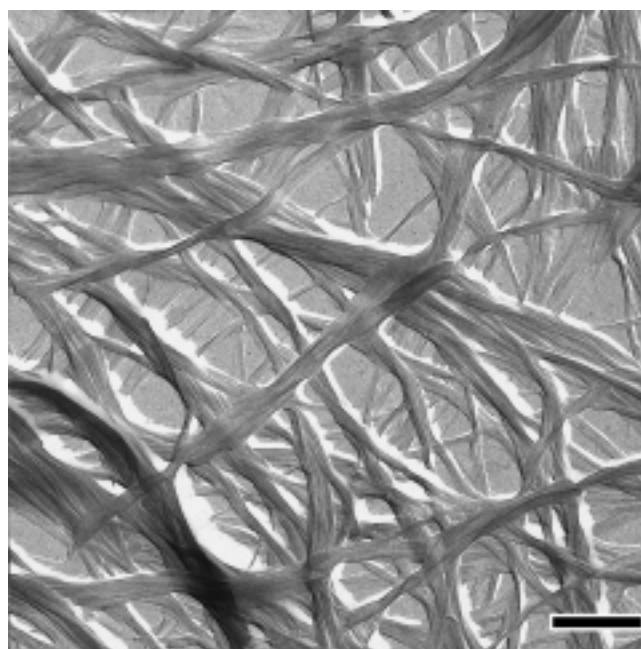


Figure 3. Electron microscopy photograph of a tetralin gel of **1** (Pt shadowing, bar is 500 nm).

the fibres most likely results from a strongly anisotropic growth process, and indicates that the intermolecular interactions are highly directional.<sup>[15]</sup> Electron microscopy of the

various precipitates of **2** revealed that these precipitates consist of many relatively short crystallites.

**FT-IR experiments:** The relationship between gelating ability and intermolecular hydrogen bonding was studied by means of FT-IR spectroscopy, since the N–H stretch and the amide-I and amide-II bands of ureas generally show large shifts upon the formation of hydrogen bonds. When **1** is dissolved in 1,2-dichloroethane, we found that at low concentration (4.4 mM) there is a homogeneous solution and no gel is formed. This solution shows three absorptions at 3436 (N–H), 1690 (amide-I) and 1512 (amide-II)  $\text{cm}^{-1}$ , which are characteristic for non-hydrogen-bonded urea groups (Table 2).<sup>[16]</sup> Increasing

Table 2. FT-IR data for **1** in the solid state, in solution and in the gel state.<sup>[a]</sup>

Solvent and concentration	Absorptions [ $\text{cm}^{-1}$ ]		
	NH-stretch	Amide-I	Amide-II
$\text{CHCl}_3$ , 2.8 mM (sol)	3443	1667	1523
$\text{ClCH}_2\text{CH}_2\text{Cl}$ , 4.4 mM (sol)	3436	1690	1512
$\text{CHCl}_3$ , 47.7 mM (sol)	3340	1639	1560
$\text{ClCH}_2\text{CH}_2\text{Cl}$ , 26.8 mM (gel)	3306	1634	1562
Nujol mull	3343	1632	1561

[a] All spectra are recorded at RT.

the concentration to 26.8 mM results in the formation of a gel, and the IR spectrum of this gel showed that the urea adsorption bands are shifted towards 3306, 1634 and 1562  $\text{cm}^{-1}$ . These spectral shifts are characteristic for the presence of hydrogen-bonded urea groups, and apparently formation of a gel is accompanied by the formation of intermolecular hydrogen bonds between the urea groups. The absorptions for solid **1** (Nujol mull) are in close agreement with these data (3343, 1632, 1561  $\text{cm}^{-1}$ , respectively), and indicates that in the solid state hydrogen bonding also occurs.

Although **1** does not form gels in chloroform, it was found that aggregates do build up in this solvent (vide infra). The FT-IR spectrum of a homogeneous solution of **1** in chloroform at low concentration shows strong absorptions for the urea groups at 3443 (N–H), 1667 (amide-I) and 1523 (amide-II)  $\text{cm}^{-1}$ , and corresponds very well with values reported for *N,N'*-dialkylureas in the same solvent.<sup>[17]</sup> Increasing the concentration of **1** to 47.7 mM causes a shift of these absorptions towards 3340, 1639 and 1560  $\text{cm}^{-1}$  respectively (Table 2). These concentration-dependent spectral shifts are again indicative of the formation of aggregates stabilised by intermolecular hydrogen bonds between the urea groups.<sup>[4b, 6b]</sup>

**Molecular modelling:** Molecular modelling is a powerful tool to provide insight into the interaction potential surface of molecules and into their possible modes of aggregation, but for many known gelators the use of molecular modelling is complicated by the large degree of conformational freedom of the compounds. In order to reduce the conformational space to a minimum, geminal bis-urea **7** was chosen as a model compound for the molecular modelling experiments. The conformational space of **7** is formed by the three dihedral angles  $\phi_1$ ,  $\phi_2$  and  $\phi_3$  of the bonds connecting the urea moieties and the phenyl group with the geminal carbon atom (Figure 4a). A conformational search using the CHARMM force

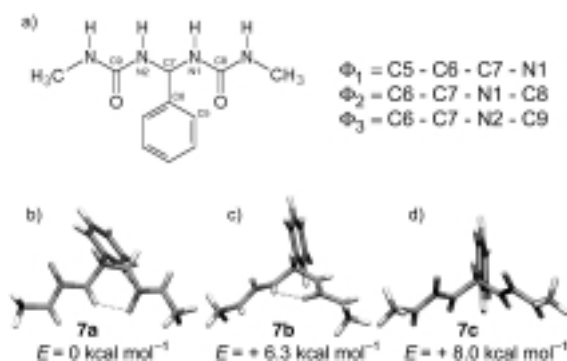


Figure 4. Dihedral angles definition (a) and calculated minimum energy and saddle point conformations of **7** (b–d).

field as implemented in Quanta97 was carried out by systematic variation of  $\phi_2$  and  $\phi_3$ , whereas no restrictions were applied to  $\phi_1$ .<sup>[18]</sup> Only one stable conformation (**7a**) was identified by this conformational search, and for symmetry reasons results in two global energy minima on the potential-energy surface formed by the dihedral angles  $\phi_2$  and  $\phi_3$ . In the minimum-energy conformation a single hydrogen bond is present between the two urea groups (Figure 4b). The rotation of the urea groups around  $\phi_2$  and  $\phi_3$  is marked by two saddle points (**7b**, **7c**, Figure 4c and 4d) which are 6.3  $\text{kcal mol}^{-1}$  and 8.0  $\text{kcal mol}^{-1}$  higher in energy.

The interaction potential surfaces of **7a–c** were explored by calculating the interaction energy between a molecule of **7** located at the centre of a cubic box with a second molecule of **7** while systematically varying the Euler angles of rotation and repeating this procedure at each point of a cubic box spaced by 0.5 Å in each direction. The interaction potential surfaces of the conformers **7a** and **7b** do not show preferential sites for complementary hydrogen-bond interactions with a second molecule. This is in large contrast with **7c**, which has a highly anisotropic interaction potential surface, with the most favourable sites of interaction being located on the axes along the urea carbonyl bonds (Figure 5). Similar results have been obtained for bis-ureas based on 1,2-diaminobenzene and 1,2-diaminocyclohexane.<sup>[6b]</sup>

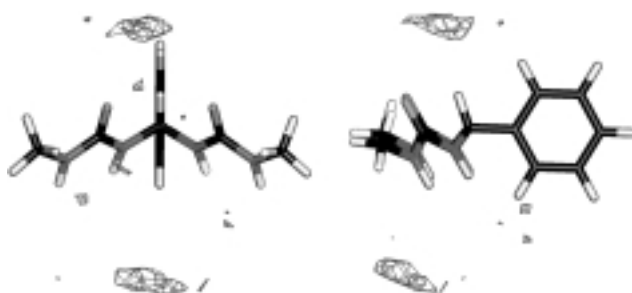


Figure 5. Interaction potential surface of conformer **7c**.

One-dimensional aggregates of **7** can then be constructed by applying the appropriate symmetry operations to the various conformers: translation ( $P1$ ), screw axis ( $P2_1$ ), glide plane ( $Pa$ ) or inversion ( $P\bar{1}$ ).<sup>[19]</sup> When these operations are carried out along an axis that runs through the most

favourable site(s) of interaction, which can be obtained from the interaction potential surface, one can expect that the most stable 1D aggregates will be formed.

In general, for bis-urea molecules in which the urea groups can be connected by any kind of linker, aggregates with *antiparallel* (*a-*) oriented hydrogen-bonded arrays of urea groups can be constructed by application of a translation (*a-P1*), glide plane (*a-Pa*) or inversion (*a-P $\bar{1}$* ) operation. Aggregates in which the hydrogen-bonded arrays of urea groups have a *parallel* (*p-*) orientation can be constructed by a translation (*p-P1*), screw axis (*p-P2 $_1$* ) or glide plane (*p-Pa*) operation (Figure 6). Evidently, a glide plane and inversion

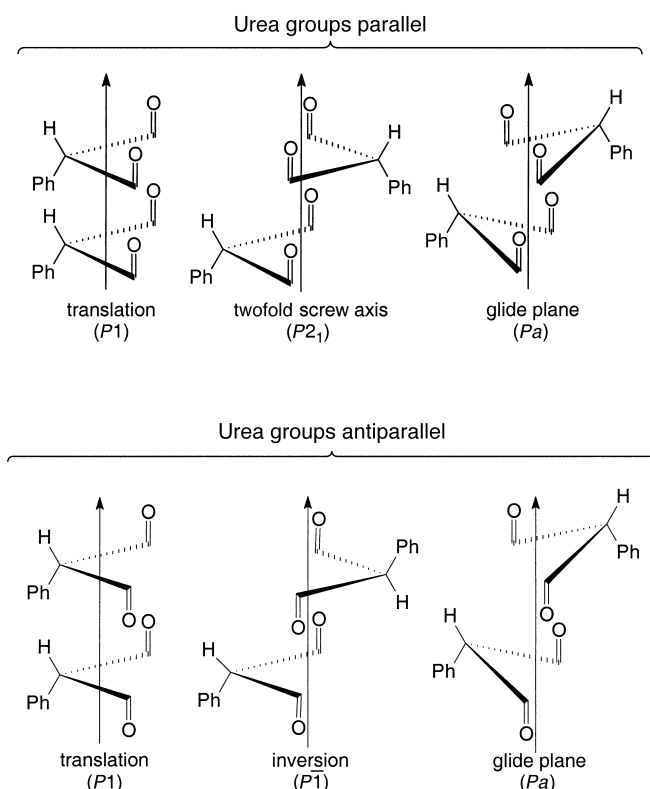


Figure 6. Symmetry-restricted aggregates of **7**. For reasons of clarity the hydrogen-bonding direction of the urea groups is indicated by the carbonyl groups only.

operation can not be used when a chiral centre is present unless one is dealing with aggregates containing both enantiomers, but this restriction does not apply to our achiral geminal bis-urea compounds.

The structures and stabilities of all these six aggregate forms were investigated by means of molecular mechanics calculations. Although no distinctive sites of interaction could be obtained for conformers **7a** and **7b** (vide supra) it was found that they do give stable one-dimensional aggregates, all with an antiparallel orientation of the urea groups, whereas the use of conformer **7c** leads to aggregates with parallel-oriented urea groups (Figure 7). The loss of the intramolecular hydrogen bond in the three conformers **7a,b** is compensated by the formation of four intermolecular hydrogen bonds between adjacent molecules. It was found that in all these

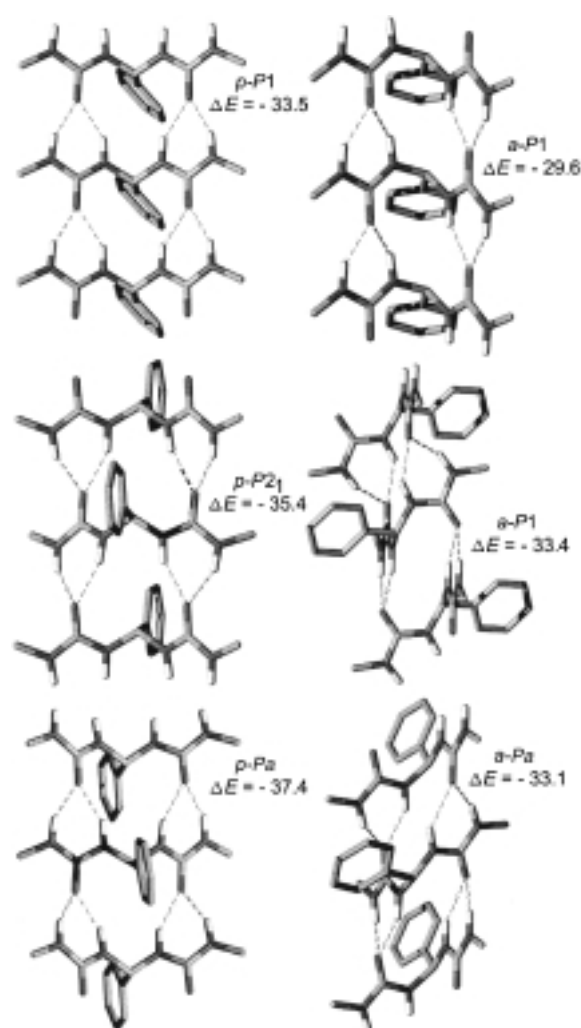


Figure 7. Symmetry-restricted one-dimensional aggregates of **7** obtained by molecular modelling. Energies (kcal mol<sup>-1</sup>) are relative to conformer **7a**.

aggregates every urea group participates completely in hydrogen bonding with an adjacent molecule.

The structures of the calculated hydrogen-bonded networks are in general in good agreement with what is found for various mono-urea derivatives in the solid state. For the translational aggregates *p-P1* and *a-P1* the repeating distances that give the lowest aggregate energies are 4.5–4.6 Å, values that are in excellent agreement with previously reported X-ray data.<sup>[20]</sup> The other aggregates contain two molecules per unit cell and give repeating distances in the range of 8.8–9.0 Å, which are also in good agreement with literature reports.<sup>[6b, 20]</sup>

A distinct feature of urea compounds is that in crystal structures the urea groups form colinear and coplanar hydrogen-bonded arrays (Figure 8). Within the *a-Pa* and *a-P $\bar{1}$*  aggregates, however, the hydrogen-bonded arrays deviate substantially from colinearity and coplanarity, with  $\alpha = 90^\circ$  and  $\beta = 28^\circ$  for *a-Pa* and  $\alpha = 95^\circ$  and  $\beta = 27^\circ$  for *a-P $\bar{1}$* . Therefore these aggregates are less likely to occur. In the aggregates with *a-P1*, *p-P1*, *p-P2 $_1$*  and *p-Pa* symmetry the urea groups form indeed colinear and coplanar hydrogen-bonded arrays. Of these aggregates, the ones with *p-P2 $_1$*  and *p-Pa*

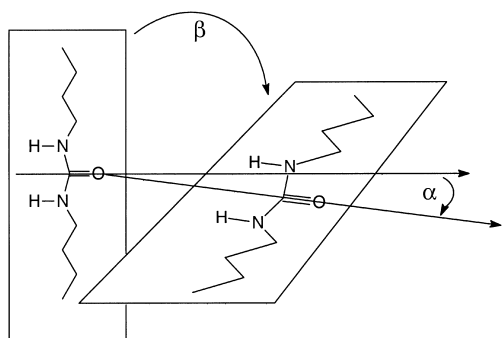


Figure 8. Colinearity angle  $\alpha$  and dihedral  $\text{N-C-O}\cdots\text{H}$  angle  $\beta$  of two hydrogen-bonded urea fragments.

symmetry are the most stable ones, indicating that an alternating orientation of successive molecules is more favourable.<sup>[20, 21]</sup>

**NMR experiments:** In general, NMR techniques can give a great deal of information on, for example, self-assembly processes in solution. Especially the use of NOESY experiments may provide an insight in to how molecules are orientated with respect to one another in an aggregated state. It was found that the geminal bis-urea compounds do not form gels in chloroform and are soluble up to a concentration of at least 78.0 mM, but the concentration-dependent infrared measurements showed that these compounds nevertheless do aggregate in this solvent (vide supra). We therefore studied the aggregation behaviour of these compounds in chloroform in more detail by using solution NMR techniques.  $^1\text{H}$  NMR measurements of compound **1** in  $\text{CDCl}_3$  showed that the spectra are extremely sensitive to changes in concentration and temperature. Concentration-dependent measurements revealed that at low concentrations ( $<0.62\text{ mM}$ ) the  $^1\text{H}$  NMR spectrum does not change significantly, but an increase of the concentration resulted in clear downfield shifts of the spectral positions of the NH protons and an upfield shift of the spectral positions of the  $\alpha\text{-CH}_2$  protons, until at higher concentration a plateau is reached (Figure 9). Apparently, at low concentra-

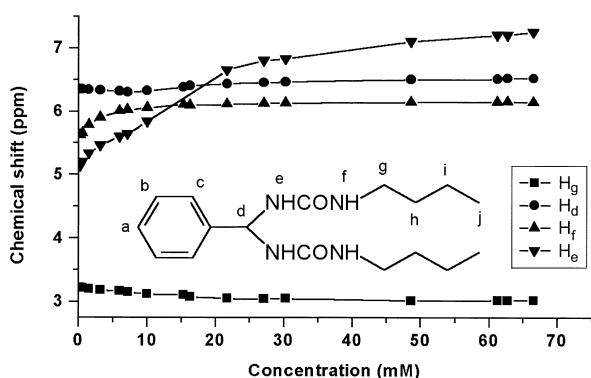


Figure 9. Concentration-dependent  $^1\text{H}$  NMR shifts of **1** in  $\text{CDCl}_3$  at room temperature.

tion **1** is mainly present as a monomer, whereas at higher concentration the equilibrium is shifted in favour of the aggregate.<sup>[22]</sup> These results are in excellent agreement with the

FT-IR data. The data in Figure 9 could not be fitted by a model which involved only the formation of dimers, and thus suggests that higher aggregates rather than dimers are involved.<sup>[23]</sup> This formation of higher aggregates is also confirmed by NOESY experiments (vide infra).

The  $^1\text{H}$  NMR spectra of **1** in  $\text{CDCl}_3$  are very sensitive to changes in temperature. Increasing the temperature for a concentrated solution (47.7 mM) of **1** causes an upfield shift of the spectral positions of the NH protons (and a downfield shift of the  $\alpha\text{-CH}_2$  protons), and indicates a return to mainly monomeric species in solution. Decreasing the temperature causes the opposite effect, and is accompanied by line-broadening of the spectra. Evidently, at higher concentrations the degree of aggregation is strongly dependent on the temperature.

At low concentrations a change of the temperature has a different effect (Figure 10). At  $25^\circ\text{C}$  and a concentration of 1.6 mM the NH(e) and NH(f) signals are broad singlets but

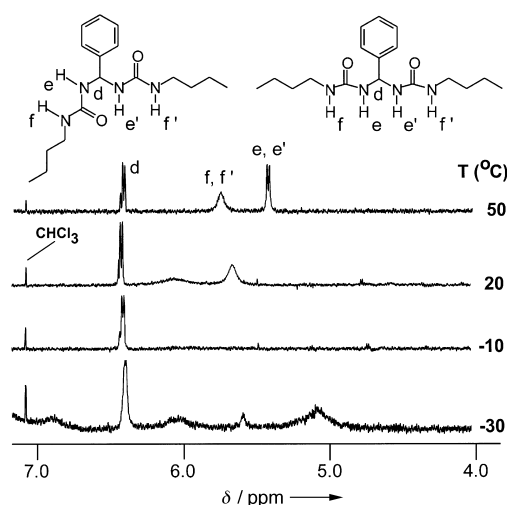


Figure 10. Temperature-dependent  $^1\text{H}$  NMR spectrum of a 1.6 mM solution of **1** in  $\text{CDCl}_3$ .

when the temperature is raised to  $55^\circ\text{C}$ , the NH(e) signal becomes a well-resolved doublet. On the other hand, decreasing the temperature results in a broadening of only the NH signals, until at  $-10^\circ\text{C}$  they disappear, but at  $-30^\circ\text{C}$  four new signals appear. Apparently, at  $-30^\circ\text{C}$  and lower all four NH protons are inequivalent, indicating that rotation around  $\phi_2$  and  $\phi_3$  (Figure 4) has become slow on the NMR time scale. These results are in excellent agreement with the molecular modelling calculations which indicate that the minimum-energy conformation lacks an element of symmetry and that this conformation is stabilised by the presence of a single intramolecular hydrogen bond. Apparently, at room temperature this intramolecular hydrogen bond becomes weak enough so that rotation around  $\phi_2$  and  $\phi_3$  becomes fast on the NMR time scale and consequently the NH protons are observed as two time-averaged signals.

Interestingly, the coupling pattern of the urea NH protons indicates that for the monomeric species the position of the NH(e) proton is upfield relative to the position of NH(f). This is confirmed by 2D NOESY (vide infra) and COSY experi-

ments. As shown in Figure 10, upon aggregation a large downfield shift of NH(e) of 1.5 ppm is observed (from 0.31 to 60.2 mM in  $\text{CDCl}_3$ ), whereas the other signals shift only by 0.2–0.5 ppm. The high-field position of the NH(e) signal relative to the NH(f) signal at low concentration and high temperature is quite remarkable and counterintuitive, since one would have expected it the other way round, based on substituent effects.  $^1\text{H}$  NMR experiments with the model compound *N*-benzyl-*N'*-octylurea showed that in this compound this is indeed the case. Most likely, the anomalous upfield position of the NH(e) proton for the monomeric species is due to shielding by the phenyl group. This is again in excellent agreement with the results from molecular modelling which showed that for the minimum-energy conformation **7a** one of the NH(e) protons is indeed located in the shielding region, and apparently also compound **1** exist predominantly in the most stable intramolecular hydrogen-bonded form both at low as well as higher temperatures. Since upon aggregate formation a significant conformational change must take place, the NH(e) proton is no longer to be found in the shielding region of the phenyl group, and consequently for the aggregated species present at high concentration the signals of the NH protons return to their 'normal' spectral positions as one would have expected based on substituent effects and the formation of hydrogen-bonded urea species. More support for this idea comes from the data obtained from  $^1\text{H}$  NMR spectra with  $[\text{D}_6]\text{DMSO}$  as a solvent. In  $[\text{D}_6]\text{DMSO}$  no aggregation takes place and intramolecular hydrogen bonding is also highly unlikely owing to the strongly hydrogen-bond accepting character of  $[\text{D}_6]\text{DMSO}$ , and this is known to disrupt inter- and intramolecular solute hydrogen bonds. In this solvent, we find for all compounds **1–6** that the signal for the NH(e) proton lies downfield with respect to the signal for NH(f), exactly what is to be expected on the basis of substituent effects.

In order to obtain more information about the structure of these aggregates, two NOESY experiments were carried out with **1** in  $\text{CDCl}_3$  at different temperatures and concentrations. At 50 °C and a concentration of 4.0 mM, the only cross peaks observed are the ones from nearest neighbour contacts, so it can be concluded that there is (almost) exclusively non-aggregated **1** in solution. Increasing the concentration to 27.2 mM at 25 °C results in a number of additional NOE cross peaks, especially between the phenyl and butyl segments of the molecule (Figure 11). It was observed that all NOE enhancements in the aggregated state are negative, whereas they are all positive in the nonaggregated state. This indicates that at this concentration and temperature the majority of the formed aggregates have a molecular weight of at least 1500 or higher, which means that these aggregates consist of at least

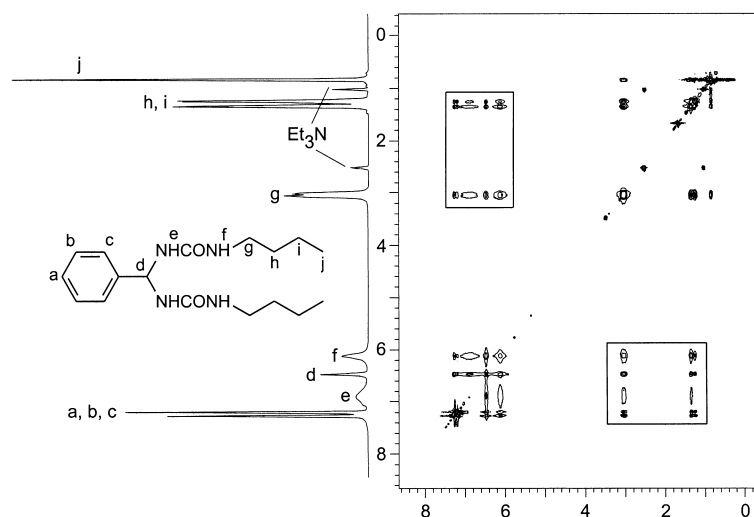


Figure 11. NOESY spectrum of **1** at a concentration of 27.2 mM in  $\text{CDCl}_3$ .

six monomeric units.<sup>[24]</sup> Apparently, the additional NOE interactions observed at high concentration correspond to intermolecular close contacts only present in the aggregate of **1**.

On the basis of the additional NOE interactions it is evident that there must be aggregates present with  $P2_1$ ,  $Pa$  or  $P\bar{1}$  symmetry (Figure 7), since only in these aggregates will there be NOE interactions between protons of the phenyl and butyl groups (Figure 12). Although on the basis of these NOESY

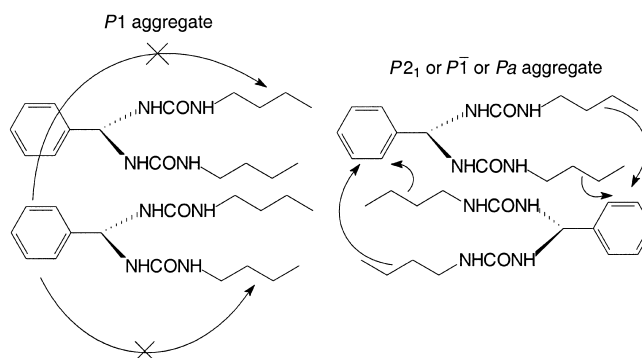


Figure 12. Explanation of NOE interactions between adjacent molecules of **1**.

experiments the presence of aggregates with  $P1$  symmetry cannot be excluded, it must be considered highly unlikely that more than one aggregate form is present, since none of the experiments that were carried out points towards polymorphism.<sup>[25]</sup>

Since the FT-IR spectroscopy results showed that hydrogen bonding also occurs in the solid state (vide supra)  $^1\text{H}$ -MAS and  $^{13}\text{C}$ -CP/MAS NMR experiments were carried out in order to establish a relationship between the aggregated species in solution ( $\text{CDCl}_3$ ), in the gel-state ( $[\text{D}_8]\text{toluene}$ ) and in the solid state.<sup>[26]</sup>

In general it was found that attempts to measure  $^1\text{H}$  NMR spectra of gels are not successful owing to excessive dipolar broadening, and  $^1\text{H}$ -MAS NMR of both the gel and the solid state gave complex and highly broadened spectra, most likely owing to dipolar interactions and spin diffusion. However, the

$^{13}\text{C}$ -CP/MAS NMR spectra are of a much better quality (Figure 13), and give well-resolved signals for both the solid state and the gel state, although the  $^{13}\text{C}$  NMR spectrum of the latter has a poor S/N ratio, due to limited experiment time.

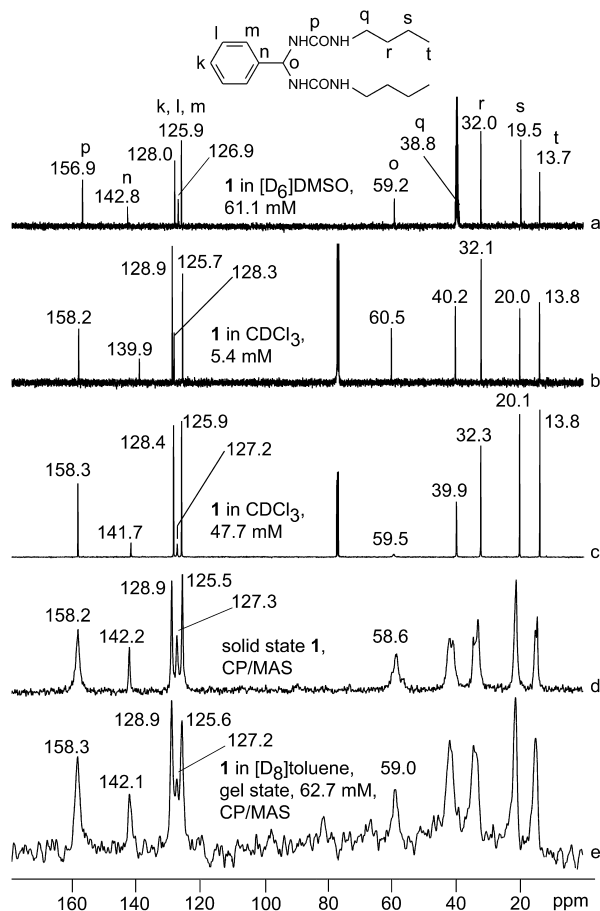


Figure 13. Comparison of solution  $^{13}\text{C}$  NMR data (a: 61.1 mM in  $[\text{D}_6]\text{DMSO}$ ; b: 5.4 mM in  $\text{CDCl}_3$ ; c: 47.7 mM in  $\text{CDCl}_3$ ) of **1** with  $^{13}\text{C}$  NMR-CP/MAS data of the solid state (d) and the gel state (e).

A comparison of **1** in  $[\text{D}_6]\text{DMSO}$  (Figure 13a), at low concentration in  $\text{CDCl}_3$  (Figure 13b), at high concentration in  $\text{CDCl}_3$  (Figure 13c), in the solid state (Figure 13d) and the gel state in  $[\text{D}_8]\text{toluene}$  (Figure 13e) reveals that the changes in the spectral positions of the various carbon atoms are less dramatic than for the corresponding proton spectral positions in the  $^1\text{H}$  NMR spectrum.

It is found that at both low and high concentration of **1** in  $\text{CDCl}_3$  (Figure 13b and 13c) the carbonyl signal (p) is at about the same position, even though at high concentration aggregates are formed. The fact that upon aggregation the carbonyl spectral position is shifted by not more than 0.1 ppm can be explained by the presence of intramolecular hydrogen bonding at low concentration, combined with additional weak hydrogen bonding between the solvent (H-bond donor) and the solute (both H-bond acceptor and donor). Apparently these combined interactions have the same effect upon the chemical shift as aggregation. In the gel and in the solid state the same spectral positions are found for the carbonyl signal, and indicates again that in the solid state hydrogen bonding

also occurs. In  $[\text{D}_6]\text{DMSO}$  (H-bond acceptor) an upfield shift of 1.3 ppm is observed. Doubling of the signals for the carbonyl carbon was not observed in solution or in the solid and gel states, suggesting that both carbonyl groups are equivalent, although in solution there is of course a fast exchange (vide supra). If the two carbonyls of **1** are equivalent in the aggregate and in the gel state, then the only possible aggregate symmetries are *p-P21* and *p-Pa* (Figure 6, 7).

For the quaternary phenyl carbon (n) a different behaviour is observed. It shifts from 142.8 ppm in  $[\text{D}_6]\text{DMSO}$  (Figure 13a) to 139.9 ppm in  $\text{CDCl}_3$  at low concentration (Figure 13b), this results mainly from going from no intra- or intermolecular hydrogen bond (in  $[\text{D}_6]\text{DMSO}$ ) to the formation of an intramolecular hydrogen bond and hence to a change of the conformation of **1**. As soon as aggregation takes place (Figure 13c and e), the signal of this quaternary carbon atom (n) shifts downfield again. In the solid state virtually the same position is found as in the gel state (Figure 13d). Furthermore, upon aggregate formation in  $\text{CDCl}_3$  (Figure 13c) the signal of the geminal carbon atom (o) shows a large line broadening. This points to a fast relaxation of this carbon atom, probably owing to the fact that upon aggregate formation the two urea dipoles are locked.

In general the chemical shifts in the solid state, gel state and high concentration in  $\text{CDCl}_3$  are almost the same, and indicates that **1** has the same conformation in these different states. In the solid state the signals of the butyl carbon atoms of **1** are clearly split, whereas this is not the case for the phenyl carbon atoms. This means that in the solid state all the phenyl groups are equivalent, but that there are two inequivalent butyl groups present. If this splitting of butyl signals also holds for the gel state whereas the phenyl signals do not split, then that would be strong evidence for an aggregate with *Pa*-like symmetry (Figure 6, 7), since in an aggregate with this symmetry the two butyl groups of **1** are inequivalent. The same is probably true in the gel state, but given the poor quality spectra this is not a hard fact. Another reason for the splitting of the signals may be found in the packing of the linear aggregates in the solid state and the gel state, which gives rise to secondary interactions that are of course not present in solution.

## Conclusion

It has been demonstrated that geminal bis-urea compounds are effective gelators for various organic solvents, and the concept of strong unidirectional intermolecular interactions is very useful for the design of new organogelators. The gels formed by these geminal bis-urea compounds have much in common with gels from cyclic bis-urea gelators previously reported by our group: gel formation takes place at very low concentrations (typically less than 15 mM) in a variety of organic solvents, and is completely thermoreversible with melting temperatures up to 115 °C. Electron microscopy showed that gel formation is due to the formation of long, intertwined fibres with widths of 30–300 nm and lengths up to 40  $\mu\text{m}$  by the bis-urea gelling agents, whereas FT-IR and  $^1\text{H}$  NMR experiments in chloroform and 1,2-dichloroethane



showed that aggregation of these geminal bis-urea compounds is accompanied by formation of intermolecular hydrogen bonds between the urea groups.

The relationship between molecular structure and aggregation ability and structure was studied in more detail by molecular modelling and NMR spectroscopy. Molecular modelling revealed that these geminal bis-urea compounds can form highly stable one-dimensional aggregates, which are stabilised by four hydrogen bonds between urea groups of adjacent molecules within the aggregate. Most interestingly, the modelling experiments also indicate that for the minimum-energy conformation of the monomer the urea moieties do not have the correct orientation for the formation of stable one-dimensional aggregates. Upon aggregation, however, a conformational change takes place which involves rotation of the urea moieties to a coplanar orientation, thereby exposing all hydrogen-bonding sites along one common direction. NMR experiments showed that such a conformational change indeed takes place upon the formation of hydrogen-bonded aggregates, and moreover, that the conformation in the aggregate and the gel state is the same.

A symmetry analysis of possible one-dimensional aggregate structures of bis-urea compounds showed that in principle a number of aggregate structures are possible, all of which are stabilised by the maximum number of hydrogen bonds between adjacent molecules. The relative stabilities of the possible aggregate structures were investigated by molecular modelling and these studies indicate that aggregates with either *p*-*P*<sub>2</sub><sub>1</sub> or *p*-*Pa* symmetry are favoured over others. The results of the NOESY NMR experiments agree well with the molecular modelling calculations: the observed intermolecular close contacts between the phenyl and butyl moieties of the geminal bis-urea compound unambiguously show the presence of aggregates with either *p*-*P*<sub>2</sub><sub>1</sub> or *p*-*Pa* symmetry, but unfortunately, they do not exclude the presence of a significant fraction of aggregates with *P*<sub>1</sub> (translation) symmetry.

These studies clearly show that molecular modelling and solution NMR studies of aggregation for organic gelling agents in combination with solid-state NMR studies can give valuable insights into gel formation and gel structure. Although at present polymorphism in solution aggregates and gels of geminal bis-ureas can not be excluded, the NMR studies point to the presence of exclusively one kind of aggregate.<sup>[27]</sup>

## Experimental Section

**Chemicals:** All compounds used (benzaldehyde, *p*-chlorobenzaldehyde, *p*-methoxybenzaldehyde, *p*-nitrobenzaldehyde, dimethylaminobenzaldehyde, butylurea, benzylurea) were commercially available (Aldrich, ACROS) and were used without further purification. Toluene and diethyl ether were distilled from sodium prior to use. Dichloromethane was distilled from P<sub>2</sub>O<sub>5</sub> prior to use. CDCl<sub>3</sub> (Aldrich) was dried and freed from traces of acid over Na<sub>2</sub>SO<sub>4</sub>/K<sub>2</sub>CO<sub>3</sub> and kept basic with some triethylamine in order to prevent decomposition of the geminal bis-urea **1** during the NMR experiments. [D<sub>6</sub>]DMSO (Aldrich) was used as received and stored over molecular sieves.

## Preparation of geminal bis-ureas

**1-Butyl-3-[(3-butylureido)phenylmethyl]urea (1):** Benzaldehyde (2.03 g, 19.1 mmol) and *n*-butylurea (4.44 g, 38.2 mmol) were suspended in toluene (125 mL). A little *p*-TsOH was added and the solution was refluxed for 3 h under Dean–Stark conditions with the exclusion of moisture from the air. During the reaction the mixture became turbid and after cooling to room temperature, a nontransparent, white gel was formed. The gel was filtered with suction over a glass filter and the residue, an off-white crusty compound, was crushed with a spatula, suspended in a 50:50 mixture of dichloromethane and diethyl ether and subjected to ultrasound in order to obtain a very finely divided suspension. This suspension was centrifuged and the white sediment was collected. This procedure was repeated twice, after which white solid **1** was obtained (4.72 g, 13.9 mmol, 73%). <sup>1</sup>H NMR (300 MHz, [D<sub>6</sub>]DMSO): δ = 0.84 (t, *J* = 7.0 Hz, 6H), 1.30 (m, 8H), 2.98 (dt, *J* = 5.9, 8.5 Hz, 4H), 6.08 (t, *J* = 8.5 Hz, 1H), 6.15 (t, *J* = 8.3 Hz, 2H), 6.58 (d, *J* = 8.3 Hz, 2H), 7.21–7.35 (m, 5H); <sup>13</sup>C NMR (75.48 MHz, [D<sub>6</sub>]DMSO): δ = 13.7, 19.5, 32.1, 38.8, 59.2, 126.1, 127.1, 128.4, 143.0, 157.1; elemental analysis: calcd (%) for C<sub>17</sub>H<sub>28</sub>N<sub>4</sub>O<sub>2</sub>: C 63.69, H 8.81, N 17.51; found: C 63.53, H 8.86, N 17.34; m.p.: > 170 °C (decomp); IR (Nujol mull):  $\tilde{\nu}_{\max}$  (cm<sup>-1</sup>): 3343 (s, N–H), 1632 (s, amide-I), 1562 (s, amide-II).

**1-Benzyl-3-[(3-benzylureido)phenylmethyl]urea (2):** This compound was prepared as described for **1**, starting from benzylurea and benzaldehyde. Yield 82%. White solid. <sup>1</sup>H NMR (300 MHz, [D<sub>6</sub>]DMSO): δ = 4.22 (d, *J* = 5.9 Hz, 4H), 6.25 (t, *J* = 8.2 Hz, 1H), 6.60 (t, *J* = 9.6 Hz, 2H), 6.80 (d, *J* = 8.1 Hz, 2H), 7.19–7.35 (m, 15H); <sup>13</sup>C NMR (75.48 MHz, [D<sub>6</sub>]DMSO): δ = 42.8, 59.4, 125.9, 126.6, 127.0, 128.1, 128.2, 140.6, 142.7, 157.0, 182.9; elemental analysis: calcd (%) for C<sub>23</sub>H<sub>22</sub>N<sub>4</sub>O<sub>2</sub>: C 71.13, H 6.22, N 14.41; found: C 71.06, H 6.16, N 14.44; m.p.: > 170 °C (decomp); IR (Nujol mull):  $\tilde{\nu}_{\max}$  (cm<sup>-1</sup>): 3337 (s, N–H), 1630 (s, amide-I), 1559 (s, amide-II).

**1-Butyl-3-[(3-butylureido)-(p-chlorophenyl)methyl]urea (3):** This compound was prepared as described for **1**, starting from butylurea and *p*-chlorobenzaldehyde. Yield 78%. White solid. <sup>1</sup>H NMR (300 MHz, [D<sub>6</sub>]DMSO): δ = 0.85 (t, *J* = 7.1 Hz, 6H), 1.19–1.36 (m, 8H), 2.97 (dt, *J* = 5.9, 8.8 Hz, 4H), 6.10 (brs, 3H), 6.64 (d, *J* = 8.1 Hz), 7.30 (d, *J* = 8.4 Hz, 2H), 7.37 (d, *J* = 8.4 Hz, 2H); <sup>13</sup>C NMR (75.48 MHz, [D<sub>6</sub>]DMSO): δ = 13.7, 19.5, 32.0, 38.8, 58.7, 127.9, 127.9, 131.4, 142.0, 157.0; elemental analysis: calcd (%) for C<sub>17</sub>H<sub>27</sub>ClN<sub>4</sub>O<sub>2</sub>: C 57.50, H 7.70, N 15.80; found: C 57.53, H 7.71, N 15.68; m.p.: > 170 °C (decomp); IR (Nujol mull):  $\tilde{\nu}_{\max}$  (cm<sup>-1</sup>): 3331 (s, N–H), 1638 (s, amide-I), 1562 (s, amide-II).

**1-Butyl-3-[(3-butylureido)-(p-methoxyphenyl)methyl]urea (4):** This compound was prepared as described for **1**, starting from butylurea and *p*-methoxybenzaldehyde. Yield 65%. White solid. <sup>1</sup>H NMR (300 MHz, [D<sub>6</sub>]DMSO): δ = 0.85 (t, *J* = 7.1 Hz, 6H), 1.22–1.36 (m, 8H), 2.97 (dt, *J* = 6.2, 9.3 Hz, 4H), 3.72 (s, 6H), 6.04–6.11 (m, 3H), 6.50 (d, *J* = 8.4 Hz, 2H), 6.87 (d, *J* = 8.8 Hz, 2H), 7.21 (d, *J* = 8.8 Hz, 2H); <sup>13</sup>C NMR (75.48 MHz, [D<sub>6</sub>]DMSO): δ = 13.7, 19.5, 32.1, 38.8, 55.1, 58.8, 113.4, 127.1, 134.8, 157.0, 158.3; elemental analysis: calcd (%) for C<sub>18</sub>H<sub>30</sub>N<sub>4</sub>O<sub>2</sub>: C 61.70, H 8.61, N 16.03; found: C 61.74, H 8.51, N 15.90; m.p.: > 170 °C (decomp); IR (Nujol mull):  $\tilde{\nu}_{\max}$  (cm<sup>-1</sup>): 3345 (s, N–H), 1638 (s, amide-I), 1568 (s, amide-II).

**1-Butyl-3-[(3-butylureido)-(p-dimethylaminophenyl)methyl]urea (5):** This compound was prepared as described for **1**, starting from butylurea and *p*-dimethylaminobenzaldehyde. Yield 48%. White solid. Purification of this compound was very difficult (see elemental analysis) because of its instability. It decomposes rapidly to the starting materials, as was noted by the always present smell of the parent aldehyde. NMR spectroscopy reveals that, after purification, the compound is at least of 90% purity. <sup>1</sup>H NMR (300 MHz, [D<sub>6</sub>]DMSO): δ = 0.87 (t, *J* = 7.1 Hz, 6H), 1.27–1.41 (m, 8H), 2.85 (s, 6H), 2.97 (d, *J* = 5.5 Hz, 4H), 6.05 (brs, 3H), 6.40 (d, *J* = 8.1 Hz, 2H), 6.67 (d, *J* = 8.1 Hz, 2H), 7.11 (d, *J* = 8.1 Hz, 2H); <sup>13</sup>C NMR (75.48 MHz, [D<sub>6</sub>]DMSO): δ = 13.7, 19.5, 32.1, 38.8, 40.3, 58.9, 112.1, 121.7, 130.3, 149.7, 157.0; elemental analysis: calcd (%) for C<sub>19</sub>H<sub>33</sub>N<sub>5</sub>O<sub>2</sub>: C 62.80, H 9.20, N 19.30; found: C 59.88, H 8.78, N 18.57; m.p.: > 170 °C (decomp); IR (Nujol mull):  $\tilde{\nu}_{\max}$  (cm<sup>-1</sup>): 3337 (s, N–H), 1630 (s, amide-I), 1559 (s, amide-II).

**1-Butyl-3-[(3-butylureido)-(p-nitrophenyl)methyl]urea (6):** This compound was prepared as described for **1**, starting from butylurea and *p*-nitrobenzaldehyde. Yield 79%. White solid. <sup>1</sup>H NMR (300 MHz, [D<sub>6</sub>]DMSO): δ = 0.85 (t, *J* = 7.1 Hz, 6H), 1.22–1.36 (m, 8H), 2.98 (dt, *J* = 6.2, 9.3 Hz, 4H), 6.15–6.22 (m, 3H), 6.82 (d, *J* = 8.1 Hz, 2H), 7.54 (d, *J* = 8.4 Hz, 2H), 8.20 (d, *J* = 8.4 Hz, 2H); <sup>13</sup>C NMR (75.48 MHz, [D<sub>6</sub>]DMSO):

$\delta = 13.7, 19.5, 32.0, 38.8, 58.9, 123.2, 127.2, 146.4, 150.9, 157.0$ ; elemental analysis: calcd (%) for  $C_{17}H_{27}N_3O_4$ : C 55.92, H 7.39, N 19.42; found: C 55.89, H 7.24, N 19.16; m.p.:  $>170^\circ\text{C}$  (decomp); IR (Nujol mull):  $\tilde{\nu}_{\text{max}}$  ( $\text{cm}^{-1}$ ): 3352 (s, N–H), 1640 (s, amide-I), 1580 (s, amide-II).

**Molecular modelling:** Molecular modelling calculations were carried out using the CHARMM 23 force field as implemented in Quanta97/CHARMM, a product of Molecular Simulations Inc., San Diego, USA. All calculations were carried out in the gas phase with a dielectric constant of 1. For the non-bonding interactions a cut-off radius of  $15 \text{ \AA}$  was used with a switch function working from 11 to  $14 \text{ \AA}$ . Template charges were used and all energy terms were included, with the exception of an explicit hydrogen-bonding term.

For the calculation of interaction maps (docking experiments) one molecule (substrate) of **7** was placed at the centre of a cube ( $15 \times 15 \times 15 \text{ \AA}^3$ ), with grid points spaced at  $0.5 \text{ \AA}$ . A second molecule (probe) was placed on a grid point and allowed to rotate with  $30^\circ$  increments around the Euler angles, whereby the interaction energy with the substrate was computed for each rotation. This procedure was repeated for each grid point, after which the interaction map could be constructed.

For calculations of the possible 1D aggregates the crystal modelling facility of Quanta97/CHARMM was used, with the application of periodic boundary conditions. One conformer of **7** is placed in a tetragonal unit cell ( $a = b \neq c$ ) in such a way that the C=O bonds of the urea groups are more or less (anti)parallel with one of the crystallographic axes (e.g.  $c$ ). Two sides of the box are kept at a constant size of  $50 \text{ \AA}$ , which is much larger than the cutoff radius for nonbonded interactions. In this way it is certain that no interaction with neighbouring molecules is taken into account in these directions. The third side of the box, which corresponds to the applied symmetry operation, is kept much smaller and is systematically varied. By doing so we only include intermolecular interaction along the  $c$  axis and thus 1D aggregation. The chosen length of this side of the box is varied from  $4.2\text{--}5.0 \text{ \AA}$  when there is one molecule per unit cell (translational symmetries  $p\text{-}P1$  and  $a\text{-}P1$ ), or from  $8.4\text{--}9.4 \text{ \AA}$  when there are two molecules per unit cell (all other symmetries), thus yielding the minimum-energy distance and optimal aggregate structure.

**Instruments:** Differential scanning calorimetry (DSC) measurements were carried out on a Perkin–Elmer DSC7 apparatus as previously described, and all FTIR spectra were recorded on a Mathtson Instruments 4020 Galaxy series FT-IR apparatus.<sup>[6b]</sup>

**Electron microscopy:** For electron microscopy a piece of the gel was deposited on a formvar/carbon coated copper grid (400 mesh) and removed after one minute, leaving some small patches of the gel on the grid. After drying at low pressure ( $<10^{-5}$  Torr) the specimen was shadowed at an angle of  $45^\circ$  with platinum. The specimen was examined in a JEOL 1200 EX transmission electron microscope operating at 80 kV. In studying the specimen, we first searched for patches of the gel to be sure that the observed structures originate from the gel. Micrographs were taken from structures at the periphery of the gel patches because here the fibres are deposited in a layer thin enough to be observed by transmission electron microscopy.

**NMR experiments:** Routine NMR spectra were recorded on a Varian VXR-300 spectrometer. All other experiments were performed on a Varian VXR-500 MHz spectrometer, with the exception of MAS-experiments, which were carried out with a Varian Unity 400 WB NMR spectrometer operating at 400 and 100 MHz for  $^1\text{H}$  and  $^{13}\text{C}$ , respectively. Chemical shifts are denoted in  $\delta$  units (ppm) relative to  $\text{CHCl}_3$  ( $^1\text{H}$ :  $\delta = 7.27$  ppm,  $^{13}\text{C}$ :  $\delta = 77.0$  ppm) or DMSO ( $^1\text{H}$ :  $\delta = 2.49$  ppm,  $^{13}\text{C}$ :  $\delta = 39.5$  ppm). 2D NOESY experiments were carried out with the following parameters: spectral width 4500 Hz; 16 transients for each FID; 512  $t_1$  increments and a  $2024 \times 2024$  data matrix; a mixing time  $t_m = 0.6$  s was used; a  $\pi/2$  shifted sine-squared weighting function was applied prior to Fourier transformation.

For solid-state experiments, a Jakobsen-design probehead was used in combination with a Sørensen heating apparatus and a Varian rotor speed control unit. The 5 mm  $\text{ZrO}_2$  spinners were spun under the magic angle with speeds of 8.9 kHz (for solids) and at 1.8 kHz (for gels) at  $30^\circ\text{C}$ .  $^{13}\text{C}$  NMR spectra were recorded after careful moulding using a recycle time of 5 s or more and gated high power decoupling (GHPD) during acquisition. Usually, the accumulation of 3000–6000 transients resulted in  $^{13}\text{C}$  spectra with appropriate signal to noise ratios. The solid state spectra in the gel state were carried out using deuterated co-solvents in order to

suppress additional solvent signals and allow the recording of  $^2\text{D } ^1\text{H}\text{--}^1\text{H}$  spectra. The deuterium signal was used for locking by tuning the  $X$ -channel on the deuterium frequency during 2D experiments.

**Gelation experiments:** In a typical gelation experiment a weighed amount (ca. 10 mg) of the bis-urea compound and 1 mL of the solvent were put in a GC vial, after which the vial was tightly sealed with a thin teflon disk and a screw cap. The vial was then heated with shaking until all the solid material had dissolved. The solution was set aside and allowed to cool to room temperature. Gelation was considered to have occurred when a homogeneous substance was obtained, which exhibited no gravitational flow.

For the determination of melting points of the gels a steel ball (150 mg) was placed on top of a gel, after which the vial was sealed. A series of these samples was placed in a stirred oil bath which was slowly heated (typically  $2\text{--}4^\circ\text{C min}^{-1}$ ), while the positions of the steel balls were observed and the temperature was simultaneously monitored with the aid of a thermocouple in one of the vials. The temperature at which the steel ball had reached the bottom of the vial was considered to be the melting point of a sample.<sup>[11]</sup>

## Acknowledgements

This research was supported by the Stichting Technische Wetenschappen (STW) and the Dutch Foundation for Scientific Research (NWO). The research of Dr. J. van Esch has been made possible in part by a fellowship of the Royal Netherlands Academy of Sciences (KNAW). The authors also wish to thank Ms. M. de Loos of the Stratingh Institute together with Prof. Dr. A. Brisson and Mr. J. van Breemen of the Biophysical Chemistry Department for their assistance with the Electron Microscopy experiments.

- [1] P. Terech, R. G. Weiss, *Chem. Rev.* **1997**, *97*, 3133–3159.
- [2] J. H. van Esch, F. S. Schoonbeek, M. de Loos, E. M. Veen, R. M. Kellogg, B. L. Feringa, *Supramolecular Science: where it is and where it is going*, NATO ASI Series, Series C: Mathematical and Physical Sciences, Vol. 527, Kluwer, **1998**, pp. 233–259.
- [3] a) G. M. Clavier, J.-F. Brugger, H. Bouas-Laurent, J.-L. Pozzo, *J. Chem. Soc. Perkin Trans. 2* **1998**, 2527; b) K. Hanabusa, Y. Maesaka, M. Kimura, H. Shirai, *Tetrahedron Lett.* **1999**, *40*, 2385–2388; c) R. Oda, I. Huc, S. J. Candau, *Angew. Chem.* **1998**, *110*, 2835–2838; *Angew. Chem. Int. Ed.* **1998**, *37*, 2689–2691; d) K. Yoza, Y. Ono, K. Yoshihara, T. Akao, H. Shinmori, M. Takeuchi, S. Shinkai, D. N. Reinhoudt, *Chem. Commun.* **1998**, 907–908.
- [4] a) K. Hanabusa, K. Shimura, K. Hirose, M. Kimura, H. Shirai, *Chem. Lett.* **1996**, 885–886; b) K. Hanabusa, M. Yamada, M. Kimura, H. Shirai, *Angew. Chem.* **1996**, *108*, 2086–2088; *Angew. Chem. Int. Ed. Engl.* **1996**, *35*, 1949–1951.
- [5] a) J. van Esch, R. M. Kellogg, B. L. Feringa, *Tetrahedron Lett.* **1997**, *38*, 281; b) J. van Esch, S. De Feyter, R. M. Kellogg, F. De Schryver, B. L. Feringa, *Chem. Eur. J.* **1997**, *3*, 1238–1243.
- [6] a) M. de Loos, J. van Esch, I. Stokroos, R. M. Kellogg, B. L. Feringa, *J. Am. Chem. Soc.* **1997**, *119*, 12675–12676; b) J. H. van Esch, F. S. Schoonbeek, M. de Loos, H. Kooijman, R. M. Kellogg, B. L. Feringa, *Chem. Eur. J.* **1999**, *5*, 937–950.
- [7] C. M. Snijder, J. C. De Jong, A. Meetsma, F. van Bolhuis, B. L. Feringa, *Chem. Eur. J.* **1995**, *1*, 594–597.
- [8] F. M. Menger, Y. Yamasaki, K. K. Catlin, T. Nishimi, *Angew. Chem.* **1995**, *107*, 616–618; *Angew. Chem. Int. Ed. Engl.* **1995**, *34*, 585–586.
- [9] U. Zehavi, D. Ben-Ishai, *J. Org. Chem.* **1961**, *26*, 1097–1101.
- [10] a) J. Jadzyn, M. Stockhausen, B. Zywucki, *J. Phys. Chem.* **1987**, *91*, 754–757; b) A. J. Doig, D. H. Williams, *J. Am. Chem. Soc.* **1992**, *114*, 338–343.
- [11] A. Takahashi, M. Sakai, T. Kato, *Polym. J.* **1980**, *12*, 335–341.
- [12] C. M. Garner, P. Terech, J.-J. Allegraud, B. Mistrot, P. Nuygen, A. de Geyer, D. Rivera, *J. Chem. Soc. Faraday Trans.* **1998**, *94*, 2173–2179.
- [13] K. Murata, M. Aoki, T. Suzuki, T. Harada, H. Kawabata, T. Komori, F. Ohseto, K. Ueda, S. Shinkai, *J. Am. Chem. Soc.* **1994**, *116*, 6664–6676.
- [14] Evaluation of the temperature dependence of the critical aggregation concentrations or the solubility by means of a phase-separation model or Schraders equation is only justified when the exact solute

- concentration at the melting temperature is known. Apparently, in this case the melting process is not completed, and hence the solute concentration at the melting point as determined by the dropping ball method is not equal to the given concentration.
- [15] a) P. Hartman, P. Bennema, *J. Cryst. Growth* **1980**, *49*, 145–156; b) I. Weissbuch, R. Popovitz-Biro, M. Lahav, L. Leiserowitz, *Acta Crystallogr. Sect. B* **1995**, *51*, 115–148.
- [16] J. Cz. Dobrowolsky, M. H. Jamróz, A. P. Mazurek, *Vibr. Spectrosc.* **1994**, *8*, 53.
- [17] The amide-I absorption for **1** at low concentration in chloroform shows a quite large deviation ( $23\text{ cm}^{-1}$ ) from the value for **1** at low concentration in dichloroethane. This is most likely due to the fact that chloroform acts as a hydrogen-bond donor: a) Y. Mido, *Spectrochim. Acta* **1973**, *29A*, 431–438; b) E. I. Harnagea, P. W. Jagodzinski, *Vibr. Spectrosc.* **1996**, 169.
- [18] Quanta97/CHARMm is a product of Molecular Simulations Inc., San Diego, USA. Internet: <http://www.msi.com>.
- [19] a) R. P. Scaringe, S. Perez, *J. Phys. Chem.* **1987**, *91*, 2394–2403; b) J. Perlstein, *J. Am. Chem. Soc.* **1994**, *116*, 11420–11432; c) J. W. Lauher, Y.-L. Chang, F. W. Fowler, *Mol. Cryst. Liq. Cryst.* **1992**, *211*, 99–109.
- [20] a) Y.-L. Chang, M.-A. West, F. W. Fowler, J. W. Lauher, *J. Am. Chem. Soc.* **1993**, *115*, 5991–6000; b) W. Kolodziejski, I. Wawer, K. Wozniak, J. Klinowski, *J. Phys. Chem.* **1993**, *97*, 12147–12152; c) A. J. Carr, S. J. Melendez, S. J. Geib, A. D. Hamilton, *Tetrahedron Lett.* **1997**, *39*, 7447–7450; d) C. L. Schauer, E. Matwey, F. W. Fowler, J. W. Lauher, *J. Am. Chem. Soc.* **1997**, *119*, 10245–10246; e) X. Zhao, Y.-L. Chang, F. W. Fowler, J. W. Lauher, *J. Am. Chem. Soc.* **1990**, *112*, 6627–6634.
- [21] An examination of 27 crystal structures of noncyclic urea compounds deposited in the Cambridge Crystallographic Database revealed that the carbonyl groups of adjacent urea fragments participating in hydrogen bonding are most likely to be colinear (angle  $\alpha$ , Figure 9). In addition to that, the dihedral N–C–O $\cdots$ H angle (angle  $\beta$ , Figure 9) is either (close to)  $0^\circ$  (24 cases) or (close to)  $90^\circ$  (3 cases).
- [22] The same is observed for *N,N'*-dimethylurea, only at much higher concentrations (0.2–1.0 M): K. A. Haushalter, J. Lau, J. D. Roberts, *J. Am. Chem. Soc.* **1996**, *118*, 8891–8896.
- [23] R. Deans, G. Cooke, V. M. Rotello, *J. Org. Chem.* **1997**, *62*, 836–839.
- [24] The fact that a NOE enhancement can be either positive or negative (or even zero) has to do with the correlation time of tumbling of the molecule or, in this case, the aggregate and hence is related to the size. Any advanced textbook on NOE NMR spectroscopy will provide a thorough explanation. See for example: D. Neuhaus and M. P. Williamson, *The Nuclear Overhauser Effect*, VCH, Weinheim, **1989**, pp. 31–39.
- [25] There are bis-urea compounds that form different types of aggregates in the same solution, but in these cases NMR experiments show distinctive signals for the different types of aggregates: E. M. Veen, J. van Esch, R. M. Kellogg, B. L. Feringa, unpublished results.
- [26] a) M. D. Sefcik, J. Schaefer, E. O. Stejskal, R. A. McKay, *Macromolecules* **1980**, *13*, 1132–1137; b) H. Schönherr, P. J. A. Kenis, J. F. J. Engbersen, S. Harkema, R. Hulst, D. N. Reinhoudt, G. J. Vancso, *Langmuir* **1998**, *14*, 2801–2809.
- [27] It is expected that the spectral characteristics of translational  $P1$  aggregates are different from those of  $P2_1$  and  $Pa$  aggregates. However, highly resolved spectra are only obtained in solution, under the conditions of fast exchange. In the solid state no exchange takes place, but the resolution is, in these cases, drastically reduced.

Received: October 8, 1999 [F2078]